High-Resolution NIR Imaging of Galactic Nuclei with SHARP

R. GENZEL, A. ECKART, R. HOFMANN, A. QUIRRENBACH, B. SAMS and L. TACCONI-GARMAN, Max-Planck-Institut für Extraterrestrische Physik, Garching

High-resolution imaging from the ground is substantially easier in the infrared than at visible wavelengths. The seeing-limited angular resolution decreases with wavelength λ as $\lambda^{-1/5}$ or faster, the coherence time of the atmosphere increases with $\lambda^{6/5}$ or more, and the isoplanatic angle θ, over which the phase distribution is constant, increases with $\lambda^{6/5}/H$, with H being the distance of the turbulence layer. With the recent advent of large-format, low-noise detector arrays it has now become possible to fully exploit these natural advantages of the $\lambda \geq 1\,\mu$m wavelength range.

Several techniques have been employed for achieving high angular resolution in the near-infrared. Direct, long-exposure observations typically result in about 1″ resolution, but exceptional data with 0.5″ resolution have been reported in very good seeing. If individual speckles can be seen with short exposures, diffraction-limited images can be obtained (0.15″ at 2 μm with a 3.5-m telescope). Various reconstruction techniques have been employed, ranging from the simple shift-and-add (SSA) algorithm (recentring each short exposure frame on the brightest speckle of a bright compact feature in the brightness distribution, Christou 1992) operating in the image plane, to the Knox-Thompson (Knox 1976) and triple correlation ("speckle masking": Lohmann et al. 1983) phase retrieval algorithms working in spatial frequency space. Interferometric techniques, such as non-redundant aperture masks (e.g. Haniff and Buscher 1992), have also been employed in single telescopes.

When the 256 × 256 pixel, low read noise (≤ 50 e), low dark current NICMOS 3 arrays (Rockwell International) became generally available in late 1989, we decided to put together a general-purpose, near-infrared camera for high-resolution imaging (50 milliarcsecond pixels and a 12.8 arcsecond field of view). To be able to continuously read out the array efficiently (duty cycle >70 % for the entire array at a frame rate ≤5 Hz and 2 μs per pixel) and with high speed (up to 10 Hz for single quadrant [128^2]mode) we equipped the camera with 4 fast digital signal processors (DSPs), followed by a VMS computer system. This configuration allows online, quick-look data analysis (such as SSA) which has turned out to be exceedingly useful for getting a first impression of the quality of the data and for making decisions at the telescope. This is the concept of SHARP (System for High Angular Resolution infrared Pictures) which we then proposed to the ESO Director General, Harry van der Laan, to bring to the ESO NTT as a new (guest observer) facility. A central scientific goal with SHARP on the NTT has been (and continues to be) imaging of the central stellar cluster of the Galaxy for answering the key question of whether (or not) the Galactic Centre contains a massive black hole of about $10^6\ M_\odot$. If it does, SHARP should detect proper motions of stars in the central 2 arcseconds within a time period of about 6 years. Already SHARP's first observing run in August 1991 demonstrated the capability of the new instrument and delivered a ≈ 0.25″ K-band (2.2 μm) image of the central 6″ which we reported in an earlier *Messenger* article (Eckart et al. 1991, see also Eckart et al. 1992). Subsequent observing runs delivered fully diffraction-limited (0.15″ FWHM resolution), H- (1.6 μm) and K-band images with ≈ 350 stars in the central parsec (≈25″) and ≈ 40 sources within 2″ of the dynamic centre, thus

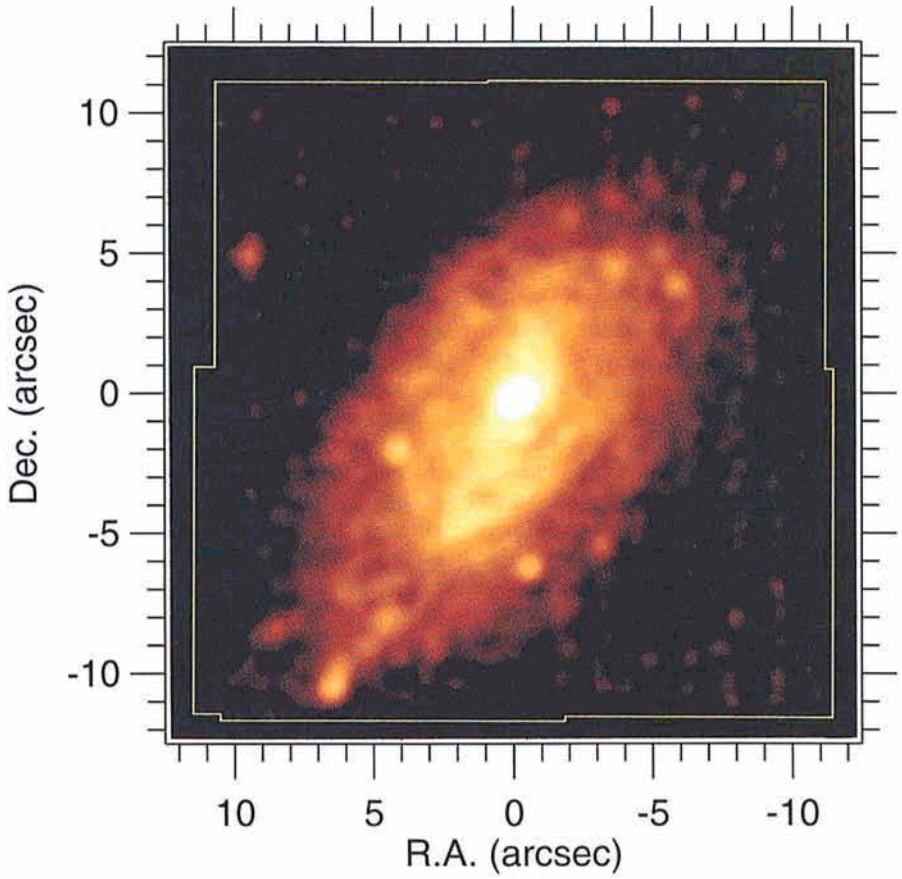

Figure 1: *0.6″ (FWHM) false-colour image of the K-band emission of NGC 1808 (Tacconi-Garman et al. 1994). The image is a mosaic of several frames and has been "Lucy"-cleaned, as described in the text. The colour table is logarithmic and the map borders (yellow lines) cover a 20″ field.*

confirming the feasibility of the proper motion experiment. These results were obtained from a combination of the shift-and-add algorithm with a "Lucy" deconvolution (Lucy 1974) as a method of obtaining high dynamic range, "CLEANed" images (Eckart et al. 1993, Genzel and Eckart 1994). SHARP has also been employed for non-redundant mask, interferometric image reconstructions. First results have been presented in the last *Messenger* (Bedding et al. 1993).

In the present article we give an overview of the first extragalactic results that have been obtained with SHARP on the NTT.

Observing Extragalactic Nuclei with SHARP

The flux density sensitivity of SHARP is determined by the read noise of the array, RN ($\approx$ 50 electrons in read-reset-read mode). Given the overall quantum efficiency-transmission product of SHARP, $\eta \approx 0.2$, and broad-band operation ($\Delta\nu/\nu = 0.2$), the 10σ flux density sensitivity for observing a "point" source in integration time per frame t on the 3.5-m NTT ($A \approx 8.2$ m^2) is

$$\Delta S(10\sigma) \approx 14\ h\nu\ RN\ N_{pix}/(\Delta\nu\ A\ \eta\ t),$$

where N_{pix} is the number of pixels over which the flux of the point source is distributed. For 50 milliarcsecond pixels and 0.5″ to 0.7″ short-integration time seeing $N_{pix} \approx 100-200$. Hence, with $t \approx 1$ second, $\Delta S(10\sigma)$ without averaging pixels is about 15 to 30 mJy, corresponding to K-band magnitude 11.5 to 12.5. For integration times $t < 1$ sec, a fraction ε of the power is still in a diffraction limited (0.15″ FWHM at 2 μm) component so that the sensitivity of diffraction-limited imaging is about $1/\varepsilon \geq 10$ times worse than $\Delta S(10\sigma)$, resulting in limited magnitudes of 9 to 10. For non-diffraction limited operation the limiting sensitivity can be further improved by either somewhat larger pixels (planned for a future version of SHARP), or by averaging pixels, or by having better seeing (a matter of telescope design and location, as well as luck). In any case this consideration already indicates that a camera with a NICMOS 3 array on a 3-m-class telescope permits, for the first time, true subarcsecond near-infrared imaging as a relatively routine matter on a number of bright nuclei. As speckles are already smeared out for integration times of about 1 second or more, the method that is employed here should be called "rapid guiding" rather than "speckle" imaging. Typically a few 10^2 to a few 10^3 frames are coadded after recentring on the brightest feature in the map. This is followed by a step of Lucy-deconvolution (or another form of "CLEAN") to correct for the wings of the point-spread function (the "seeing pedestal"), using a nearby star as deconvolution key. As a "CLEAN"-restoring beam we use a Gaussian of FWHM resolution about the same FWHM resolution as the raw recentred data. As the image is very well sampled, a modest degree of super-resolution or image sharpening (say from 0.6″ to 0.4″, depending on the source brightness) can also be achieved without too much risk and has been done for the data sets described below. The final images then have a point source sensitivity to faint structures at least an order of magnitude lower than the limit given above ($\Delta S(1\sigma$, 15 min) $\approx$ 16 to 18).

So far we have observed over a dozen compact galactic nuclei. Here we present our results on the brightest sources (Table 1).

Observations of Starburst Nuclei

Figure 1 shows a 0.6″ FWHM resolution K-band mosaic (2 array settings, Table 1, Tacconi-Garman et al. 1994) of the central 20″ (1 kpc) of the "hot spot" galaxy NGC 1808 (Sersic and Pastoriza 1965). In addition to the bright nuclear source (about 20 mJy), the circum-nuclear 2 μm emission shows two arm-like features and a number of compact knots. The data strengthen the starburst interpretation of the infrared, visible and radio emission of the galaxy (Saikia et al. 1990, Krabbe, Sternberg and Genzel 1994). The circum-nuclear near-infrared continuum emission is globally well correlated with the radio continuum and Bγ emission-line knots found by Saikia et al. and Krabbe et al., indicating that much of the near-infrared continuum emission of NGC 1808 comes from a reasonably young ($< 10^8$ years) stellar component. In particular the arm-/ridge-like structure arching east and north of the nucleus show a very good overall correlation with the radio continuum and infrared line emission there. However, on the smallest scales probed by the maps, this correlation appears to break down, as local peaks in radio continuum, Bγ and in 2 μm continuum are slightly (0.5 to 1″) displaced from each other. The prominent compact knots 6″ north-west and 10″ south-west of the nucleus do coincide with two of the visible, blueish hot spots (Véron-Cetty and Véron 1983), but then others do not. These displacements may be the result of large, local spatial variations in extinction, although the average extinction on a scale of 2″ appears to be no more than $A_V = 6$ (Krabbe et al.). Alternatively and more likely, displacements between different tracers may be the result of time evolution, considering the spatially smooth J/H/K colour distributions. The 2 μm knots may be local concentrations of red or blue supergiants (typically a few 10^2 per knot) that may be signposts of the late evolutionary stage (a few 10^7 years) of giant OB associations. Given typical velocity dispersions in molecular clouds (a few km/s), separations of 1″ or more between HII regions (Bγ and radio continuum), supernova remnants (radio continuum) and supergiants are entirely consistent with age differences of a few 10^7 years. The observations thus suggest that the central kpc of NGC 1808 currently undergoes an active phase of star formation (total rate about 10 $M_\odot$ yr^{-1}) originating (at any time) in a number of giant HII regions/OB clusters. These giant star formation complexes are probably associated with molecular clouds, may live for about one generation of OB stars and are then replaced by others bubbling up elsewhere in the disk of the galaxy.

The SHARP maps of the nearby, luminous (4×10^{10} $L_\odot$, Rieke et al. 1980) starburst galaxy NGC 253 (Fig. 2, Table 1, Sams et al. 1994) teach another lesson. While this galaxy also shows a number of prominent near-infrared hot spots in its central 150 pc, it turns out that most of these spots are not actually physical entities but merely directions of lower local extinction in a highly obscured nuclear region (Sams et al. 1994). This is evident from comparing the maps at different wavelengths (Fig. 2). The longest wavelength (K-band) map is the smoothest, while the H- and even more the J-band map show an increasing amount of structure. Mm-interferometry of the CO 1-0 line (Canzian et al. 1988) indicates that the average H_2 column density in the central 8″ is about 3×10^{22} cm^{-2} ($A_V = 20$), consistent with the ex-

TABLE 1. *Bright Galactic Nuclei Observed with SHARP*

Galaxy	Distance [Mpc]	Number of Frames	t (Frame) [secs]	FWHM Resolution	Linear Resolution
NGC 253	2.5	300 (J/H/K)	5	0.5″	6 pc
NGC 1808	10.9	200–1000 (J/H/K)	4	0.6″	31 pc
NGC 1068	14	10300 (K)	0.5–1	0.2″–0.4″	14–27 pc
NGC 7469	66	5000 (K) 700 (J/H)	1–2	0.4″	130 pc

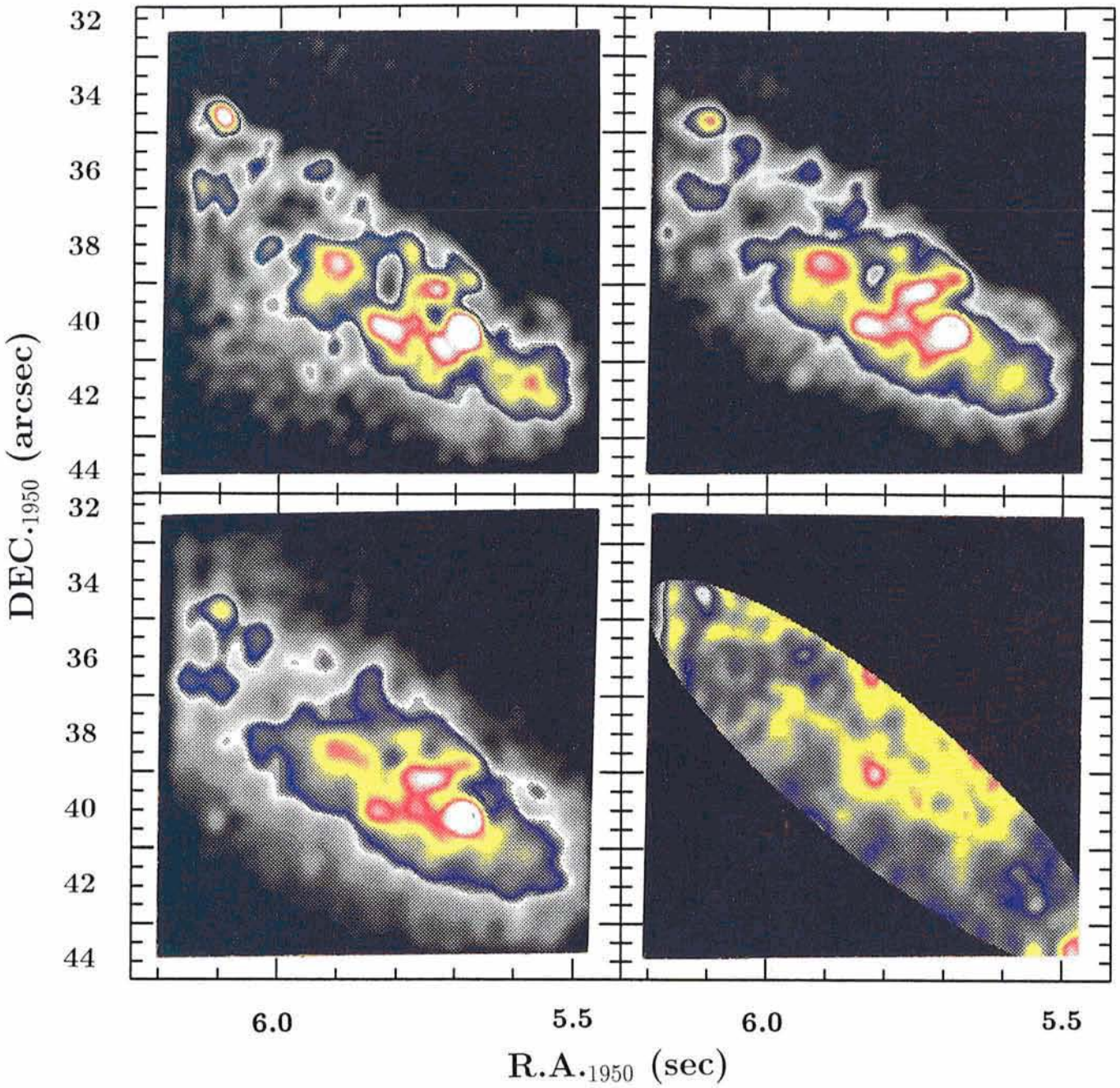

Figure 2: *0.5″ (FWHM) false-colour "Lucy"-cleaned images of NGC 253 in the J-band (1.2 μm, top left), H-band (1.6 μm, top right), K-band (2.2 μm, bottom left) and J-K colour (bottom right) (from Sams et al. 1994). Each tick on the Dec-axis is 0.5″, each tick on the R.A.-axis is 1.55″. The colour table is linear.*

tinction values required to explain the structure in the near-infrared continuum maps (Sams et al. 1994). While it is difficult to obtain detailed quantitative estimates of the dust extinction from the near-infrared data because of the uncertain relative locations of emitters and absorbers, the near-infrared colour map shown in Figure 2 is a good qualitative indicator of the (clumpy) spatial distribution of dust (and gas) on sub-arcsecond scales. Sams et al. find that the most prominent extinction peak (identical with the local "hole" of 1.2 μm emission 2″ north-east of the intensity maximum) is associated with the radio nucleus of NGC 253 and that the extinction map is globally well correlated with the radio map of Antonucci and Ulvestad (1988). In contrast to most other emission peaks on the near-infrared maps, the brightest K-band peak (≈ 15 mJy at K) does appear to be more than a direction of low extinction, namely a concentration of hot dust. Clearly, the effect of dust mixed with the stars may have an important effect on the near-infrared brightness distribution in a number of starburst nuclei, and near-infrared colour maps are a useful tool to detect and map out the absorbing dust.

Active Galactic Nuclei

Figures 3 and 4 show ≈ 0.4″ resolution near-infrared maps of two of the active galactic nuclei that have been studied with SHARP, NGC 1068 and NGC 7469. For SHARP results on the Seyfert 1/QSO I Zw 1 see Eckart et al. (1994). The near-infrared emission from NGC 1068 (Fig. 3) is characterized by the bright (500 mJy at 2.2 μm, $\geq 1.5 \times 10^{11}$ $L_{\odot}$) Seyfert 2 nucleus, plus a stellar bar at position angle 45° extending to radii of about 16″ (1 kpc at 14 Mpc). The high-resolution data now suggest that at radii larger than about 7″

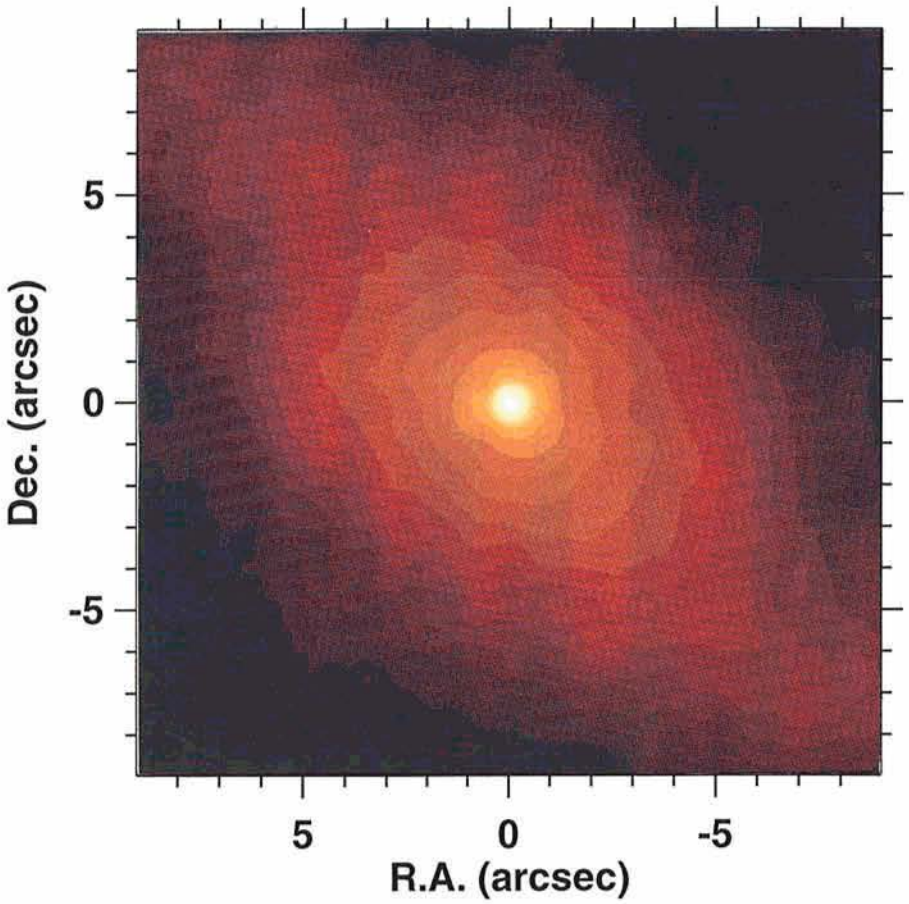

Figure 3: *0.4″ (FWHM) false-colour image of the K-band emission of the central (17.9″)² of NGC 1068 (from Quirrenbach et al. 1994). With the exception of the bright nucleus the map has not been "Lucy"-cleaned, in order to emphasize the faintest (K≈17) extended structures. The colour table is logarithmic.*

the oval bar structure (minor to major axis ratio ≈0.7) turns into two arm-like features. This radius is coincident with the inner radius of the circum-nuclear gas/dust/star formation ring (e.g. Telesco and Decher 1988), suggesting an interpretation in terms of spiral arms that have formed at the inner Lindblad resonance near the end point of the bar. The high-resolution near-infrared data also probe the radial brightness distribution, and hence, the density distribution of the stellar light very close to the Seyfert nucleus. A first-order analysis of the Data in Figure 3 (Quirrenbach et al. 1994) suggests that the 2 μm stellar light may have an effective core (half peak intensity) radius of $r_c = 2 \pm 1''$. While the brightness distribution along the major axis (p.a. 45°) and minor axis (p.a. 135°) of the bar can be well fitted by a power law of exponent $\alpha = -0.95$ and -1.65, respectively, at $r > r_c$ the distribution very close to the nucleus appears to be significantly flatter. This is a fairly difficult measurement to make quantitatively, as the brightness of the stellar bar at r=1″ is only $10^{-2.5}$ of the nuclear source. At face value this finding suggests that the 2 μm stellar light is dominated by the large scale ($\approx 10^2$ pc) disk/bar and that there is no bright, nuclear stellar cluster on a scale ≥ 30 pc. The SHARP data also confirm earlier proposals that the nuclear source has an intrinsic diameter ≤0.1″ (7 pc) and is dominated by hot dust emission. The J/H/K flux density spectrum can be described by a power law ($S \approx \nu^{-3.7}$). It is an interesting question for future research what the nature of this dust source is and whether it could be associated with the putative parsec-scale, dust/molecular torus. The near-infrared peak is displaced 0.4″ SW of the centroid of the visible emission (Gallais 1991). There is also a compact 2 μm H_2 line emission source at about the same position (Blietz et al. 1993) but mid-infrared imaging (Cameron et al. 1993) shows that most of the warm circum-nuclear dust is associated with the narrow line region.

While the extended emission in NGC 1068 is dominated by a bar-like structure, the Seyfert 1 galaxy NGC 7469 ($\geq 3 \times 10^{11} L_\odot$) exhibits a ring. Figure 4

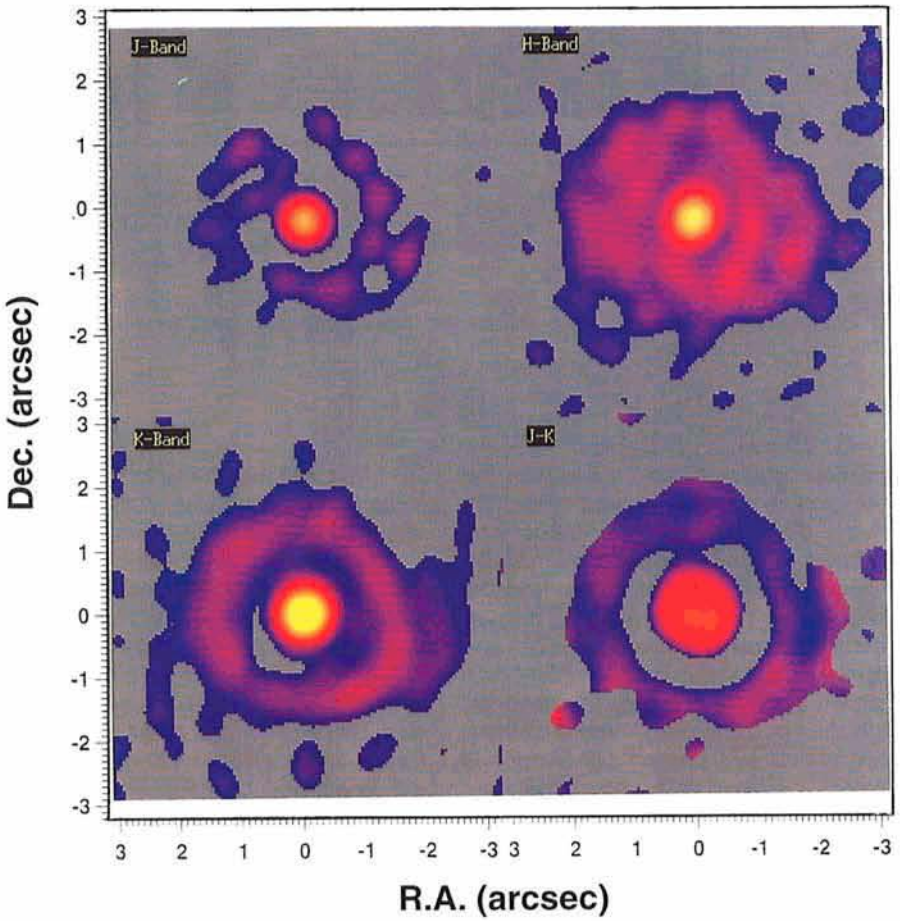

Figure 4: *0.4″ (FWHM) false-colour, "Lucy"-cleaned images of NGC 7469 in the J-band (top left), H-band (top right) and K-band (bottom left) emission, with logarithmic colour tables. The bottom right contains a 0.6″ (FWHM) J-K colour map (from Tacconi-Garman et al. 1993). Each image covers a 6.4″×6.4″ field.* *See also page 36 of this issue.*

shows the 0.4″ J/H/K SHARP images (Table 1), as well as a 0.6″ J-K colour map (Tacconi-Garman et al. 1993, Genzel et al. 1994). Outside of the Seyfert nucleus (90 mJy at K) there is a 1.5″ radius, ring structure with embedded knots. The colours of the ring are consistent with a stellar cluster reddened by $A_V \approx$ a few; in contrast, the very red nuclear colours suggest hot dust emission, as in the case of NGC 1068. The near-infrared images of Figure 4 are in very good agreement with similar resolution visible speckle images (Mauder et al. 1994) and with a VLA map of the 5 GHz radio emission (Wilson et al. 1991). All these data and $\approx 0.9''$ near-infrared spectral line imaging with the MPE FAST spectrometer fit a model in which the $\approx$500 pc ring is powered by a luminous starburst forming about 50 $M_\odot$ of new stars per year for the last 1 to 3×10^7 years (Weitzel et al. 1994). One supernova explosion every two years is implied and may be detectable by means of time variability in the high-resolution near-infrared maps. The triggering mechanism for the circum-nuclear burst in NGC 7469 remains unclear as, in contrast to NGC 1068, the SHARP data do not show evidence of a bar structure. Perhaps the burst was triggered by the interaction of NGC 7469 with its neighbour, IC 5283.

The data we have presented in this report only represent a selection of a sample of about a dozen galaxies that have been observed so far with SHARP. We believe that this brief glimpse already demonstrates the power of the new tool of subarcsecond near-infrared imaging. The future is clearly bright.

Acknowledgements. We would like to thank Harry van der Laan for giving us the opportunity to bring SHARP to the right place at the right time.

References

Antonucci, R.R.J. and Ulvestaad, J.S. 1988, *Ap.J.* **330**, L97.
Bedding, T.R., von der Lühe, O., Zijlstra, A.A., Eckart, A. and Tacconi-Garman, L. 1993, *The Messenger* **74**, 2.
Blietz, M. et al. 1994, *Ap.J.* **421**, in press.
Cameron, M. et al. 1993, *Ap.J* **419**, 136.
Canzian, B., Mundy, L.G. and Scoville, N.Z. 1988, *Ap.J.* **333**, 157.
Christou, J.C. 1991, *Exp. Astr.* **2**, 27.
Eckart, A., Hofmann, R., Duhoux, P., Genzel, R. and Drapatz, S. 1991, *The Messenger* **65**, 1.
Eckart, A., Genzel, R., Krabbe, A., Hofmann, R., van der Werf, P.P. and Drapatz, S. 1992, *NATURE* **335**, 526.
Eckart, A., Genzel, R., Hofmann, R., Sams, B.J. and Tacconi-Garman, L.E. 1993, *Ap.J.* **407**, L77.
Eckart, A., van der Werf, P.P., Hofmann, R. and Harris, A.I. 1994, *Ap.J.* April issue.
Gallais, P. 1991, PhD Thesis (Paris: University of Paris).
Genzel, R. and Eckart, A. 1994, in *Infrared Astronomy with Arrays* (3), ed. I. McLean and G. Brims (Dordrecht: Kluwer), in press.
Genzel, R. et al. 1994, in prep.
Haniff, C.A. and Buscher, D.F. 1992, *J.Opt. Soc.Am.* **9**, 203.
Knox, K.T. 1976, *J.Opt.Soc.Am.* **66**, 1236.
Krabbe, A., Sternberg, A. and Genzel, R. 1994, *Ap.J.* in press.
Lohmann, A.W., Weigelt, G. and Wirnitzer, B. 1983, *Appl.Opt.* **22**, 4028.
Lucy, L.B. 1974, *A.J.* **79**, 745.
Mauder, W., Weigelt, G., Appenzeller, I. and Wagner, S.J. 1994, *Astr.Ap.* in press.
Rieke, G.H., Lebofsky, M.J., Thompson, R.I., Low, F.J. and Tokunaga, A.T. 1980, *Ap.J.* **238**, 24.
Saikia, D.J. et al. 1990, *MNRAS* **245**, 397.
Sams, B.J., Genzel, R., Eckart, A., Tacconi-Garman, L.E. and Hofmann, R. 1994, *Ap.J.* (Lett.) in press.
Sersic, J.L. and Pastoriza, M. 1965, *PASP* **77**, 287.
Tacconi-Garman, L.J., Eckart, A., Genzel, R. and Sternberg, A., 1993, *BAAS* **25**, 1338.
Tacconi-Garman, L.J. et al. 1994, in prep.
Telesco, C. and Decher, R. 1988, *Ap.J* **334**, 573.
Véron-Cetty, M.-P. and Véron, P. 1983, *The Messenger* **34**, 22.
Weitzel, L. et al. 1994, in prep.
Wilson, A.S., Helfer, T.T., Haniff, C.A. and Ward, M.J. 1991, *Ap.J.* **381**, 79.

Infrared Spectroscopy of Galactic Globular Clusters

L. ORIGLIA[1], A.F.M. MOORWOOD[2] and E. OLIVA[3]

[1]Osservatorio Astronomico, Pino Torinese, Italy; [2]ESO; [3]Osservatorio Astrofisico, Firenze, Italy

1. Introduction

Galactic globular clusters (GGCs) are the best templates for studying the physical and chemical properties of old stellar systems at different evolutionary stages. Zinn (1985) distinguishes two main subsamples on the basis of their spatial distribution, kinematics and metallicity; the halo system characterized by low rotational velocity and metallicity ([Fe/H])≤–0.8) and large velocity dispersion, and the disk+bulge system which is metal-rich ([Fe/H])>–0.8) and exhibits a large rotational velocity and lower dispersion.

From theoretical models (Renzini and Buzzoni 1986, Chiosi et al. 1986) it is expected that the integrated luminosity of old stellar populations is dominated by the luminous red giant branch (RGB) stars which are close to the He-flash. This scenario is largely confirmed by photometric and spectroscopic optical/infrared observations of the central regions and of the brightest single stars in many clusters (see for example Frogel et al. 1983a, b and references therein). The average temperature of this red and cool stellar component, i.e. the location of the red giant branch in the HR diagram, is directly related to the metal content of the cluster; the higher [Fe/H] the cooler the stars (Frogel et al. 1983b). Therefore, any temperature sensitive index (e.g. V-K, photometric CO) could, in principle, be used to determine the metallicity of globular clusters. The main limitations in the use of photometric indexes are extinction and contamination by foreground stars and both effects are particularly important when studying high metallicity clusters in the bulge. A way to overcome these problems is to use spectroscopic indices (which are intrinsically unaffected by extinction) in the infrared where the contamination from foreground stars is much less important than in the optical. We use two spectral indices in the infrared H band centred on SiI+OH 1.59 μm and CO(6-3) 1.62 μm together with the "classical" CO(2-0) 2.29 μm feature. These indices are good temperature indicators in cool stars (Origlia et al. 1993).

In this article we present integrated spectra of these features for a sample of GGCs and show that diagrams based on their equivalent widths can be used to tightly define the metallicity sequence from metal poor halo clusters to the most metal rich in the disk+bulge.

(continued on page 23)